Acta Montanistica Slovaca
ISSN 1335-1788
actamont.tuke.sk

Validation of a Statistical Landslide Susceptibility Model for Reclamation of Closing Brown Coal Open-Cast Mines

Radka DUŽEKOVÁ [1,2], Pavel RAŠKA [2], Jan BURDA [3,5] and Jan BLAHŮT [4]*

Authors' affiliations and addresses:
[1] VUHU a.s.
tr. Budovatelu 2830/3, Most 434 01, Czechia
e-mail: radka.duzekova@gmail.com

[2] Department of Geography, Faculty of Science, J. E. Purkyně University in Ústí nad Labem, Czechia
e-mail: pavel.raska@ujep.cz

[3] VUHU a.s., tr. Budovatelu 2830/3, Most 434 01, Czechia
e-mail: burda@vuhu.cz

[4] Department of Applied Rock Mechanics, Institute of Rock Structure and Mechanics, Czech Academy of Sciences, Prague, Czechia
e-mail: blahut@irsm.cas.cz

[5] VSB Technical University Ostrava, Faculty of Mining and Geology, Ostrava, Czechia
e-mail: burda@vuhu.cz

***Correspondence:**
Pavel Raška, Department of Geography, Faculty of Science, J. E. Purkyně University, in Ústí nad Labem, Czechia
tel.: 475 286 777
e-mail: pavel.raska@ujep.cz

Funding information:
European Union
101157379 (RFCS) [MiDSafe – Advancing Post-Mining Waste Dump Safety and Sustainability].
European Union
CZ.10.02.01/00/22_002/0000210 [RUR - Region to University, University to Region].

How to cite this article:
Duželková, R., Raška, P., Burda, J. and Blahůt, J. (2026) Validation of a Statistical Landslide Susceptibility Model for Reclamation of Closing Brown Coal Open-Cast Mines. *Acta Montanistica Slovaca,* Volume 31 (1), 198-214

DOI:
https://doi.org/10.46544/AMS.v31i1.15

Abstract
Open-cast brown coal mines are being gradually closed as a result of decarbonisation policies, but the planning approaches to their reclamation and reuse have scarcely considered the potential impact of landslide hazard. We present a landslide susceptibility model and its validation for a currently closing open-cast brown coal mine in NW Czechia, one of the prominent mining regions in Europe. The model is based on a multicriteria analysis of spatial geodata applied to the 2010 landslide inventory (40 landslides with an average area of 23,400 m^2), and its accuracy was validated using a repeated landslide inventory (7 new landslides with a total area of 720,489 m^2) and a digital terrain model enabling us to detect cumulative surface deformations occurring up to 2022. Two variants of the model using different geostatistical procedures (frequency and cluster analysis) were designed and validated. The spatial fit between the mapped landslides and susceptibility classes varies due to the complex nature and retrogressive behaviour of landslides in the mining area, but validation shows an overall good fit of 2022 terrain deformation with landslide susceptibility classes in both models. Statistically significant differences ($p < 0.000$) across the susceptibility classes were found in terms of terrain deformations. Notable exception in the predictive strength of the models is the lowest susceptibility class in outside-landslide areas affected by anthropogenic modifications to a soil dump. We conclude by defining the directions for further development of the model for its use in reclamation planning.

Keywords
landslide susceptibility, open-cast brown coal mine, reclamation, statistical model

Introduction

For more than 170 years, the coal mining industry has contributed to the economic development in Europe. Hard coal and especially brown coal (lignite) mining has reshaped the landscapes and societies of many European regions, creating vast areas affected by open-cast mining, restructuring labour sectors and regional economies, and posing new developmental challenges for society (Wirth et al., 2012; Görmar et al., 2022; Pasqualetti & Frantál, 2022; Böhm et al., 2025). Yet, according to Eurostat (2022), production of brown coal in the European Union has gradually decreased since 1990, reaching 294 Mt in 2022, which is around 60% lower than in 1990. Currently, only nine countries have continued to produce brown coal in the EU, most of them from Central and Eastern Europe (Galgóczi, 2019; Eurostat, 2022). Motivated by the IPCC Special Report (IPCC, 2018) and accelerated by the European Green Deal (European Commission, 2019), the European climate policy and decarbonisation efforts are expected to result in further reduction of the production and consumption of brown coal, and therefore in the closure of open-cast mines. Many of them are already subject to reclamation and reuse (Europe Beyond Coal, 2018), which pose essential challenges of reconciling societal expectations with multiple environmental hazards present in open-cast mines. Landslides are among the most notable processes that may fundamentally limit the modes and sustainability of reuse of former open-cast brown coal mines.

However, existing approaches to assessing landslide susceptibility and related geomorphic processes have been scarcely validated in post-mining settings, and there is a fundamental lack of understanding of how these approaches and their results have been communicated to and implemented in reclamation planning practice to date. Recent studies focused on revealing landslide triggers and mechanisms related to and potentially affecting further brown coal mining operations in various types of coal mines (Burda & Vilímek, 2010; Fathi Salmi et al., 2016; Reed & Kite, 2020; Burda et al., 2022; Yang et al., 2022; Chen et al., 2023). These approaches are essential for stability analysis and for ensuring the immediate safety of mining operations at a detailed level of engineering application. For these reasons, however, these approaches have not incorporated landslide susceptibility models, which were developed mostly for non-mining regional settings (see Reichenbach et al., 2018, and Yong et al., 2022 for review). They also did not consider other human activities, which are especially relevant for post-mining development.

Some authors have already reported case studies of landslides and other geomorphic processes that affected post-mining sites after being reclaimed or left vacant (Tokgöz, 2010; Braun & Hánek, 2014; Declercq et al., 2023), thereby posing a risk to use further. The reclamation planning literature, on the other hand, provides only a general or no account of the landslide hazard affecting the reuse of post-mining sites (e.g., Kohnke, 1950; Haigh, 1992; Stottmeister et al., 2002; Karan et al., 2016; Amirshenava & Osanloo, 2018). Therefore, developing and validating landslide susceptibility models that would consider broader spatiotemporal scales of various human activities and that would be accessible to planners is needed to complement the existing risk assessments of mine closure, reclamation, and reuse (Xiao et al., 2014; Cehlár et al., 2019; Mert, 2019; Al Heib et al., 2023).

This study aims to present the landslide susceptibility model developed and validated in the open-cast brown coal mine in NW Czechia, one of the prominent brown coal mining regions in Europe. The mine is currently undergoing gradual closure and reclamation, and complex reuse of the site is planned for the next decades, while being framed by the so-called just transition efforts linked to the European Green Deal mechanisms. Our specific research aim was to validate the suitability of available spatial geodata, landslide inventories, and statistical procedures for a susceptibility model that would be capable of predicting terrain deformations on the slopes previously affected by multiple landslides.

Study area

The study area for the development and validation of the landslide susceptibility model is one of the largest open-pit coal mines located in the Most basin (Northwestern Czechia, Europe; Fig. 1). The mine is located at the contact zone between two geomorphological units: the Ore Mountains massif and the lignite Most basin (latitude 50°32'33.378"N and longitude 13°31'15.628"E). The main reason for selecting this mine was the frequent local landslides and the variety of their types, which are predisposed by specific geological conditions and triggered by anthropogenic alterations to the site. In total, the area of the mine and its dumps covers about 15 km².

The unique combination of the massif of the Ore Mountains (Krušné hory, Erzgebirge) and the geologically distinct structure of the Most Basin is the main predisposing factor for the development of extensive landslides at the margins of the mining site affected by mining operations. Knowledge of natural conditions is fundamental for producing susceptibility maps, as these conditions influence the occurrence of landslides and can serve as predictors of future events (Van Westen et al., 2008). Therefore, the most important factors will be briefly assessed in the following paragraphs. The Ore Mountains comprise orthogneisses and various crystalline rocks, while the Most Basin comprises various Cenozoic sediments dominated by Miocene claystones, a coal seam, sands, and clastic rocks (Burda & Vilímek, 2010). Since the Pliocene, both uplift of the mountain area along the Erzgebirge fault and subsidence in the basin have occurred. During the Quaternary, the upper parts were denuded, and the

mountain slopes were dissected by the river network (Bárta et al., 1973). As a result of the uplift, the contact between these two physiographic provinces is characterised by numerous slope failures occurring over the Miocene, Pleistocene, and late Holocene (Zmítko, 1983; Burda et al., 2018). Problematic zone in terms of stability is the overlying clays, which have been locally affected by the Pleistocene freeze-thaw cycles to depths of up to 60 m, thus weakening their mechanical properties. This zone is known as the regelation zone and is associated with shear surfaces of deep-seated landslides. The south-eastern slopes of the Ore Mountains rise steeply above the Most Basin, while to the northwest they continue with a gentle inclination towards the Central Saxon Upland. The elevation of the mountain massif above the surface of the basin is about 500 m. The general inclination of the slopes towards the basin is 15–35°, but it can locally reach 70°, where the crystalline rocks sink below the basin sediments (Malkovský, 1985).

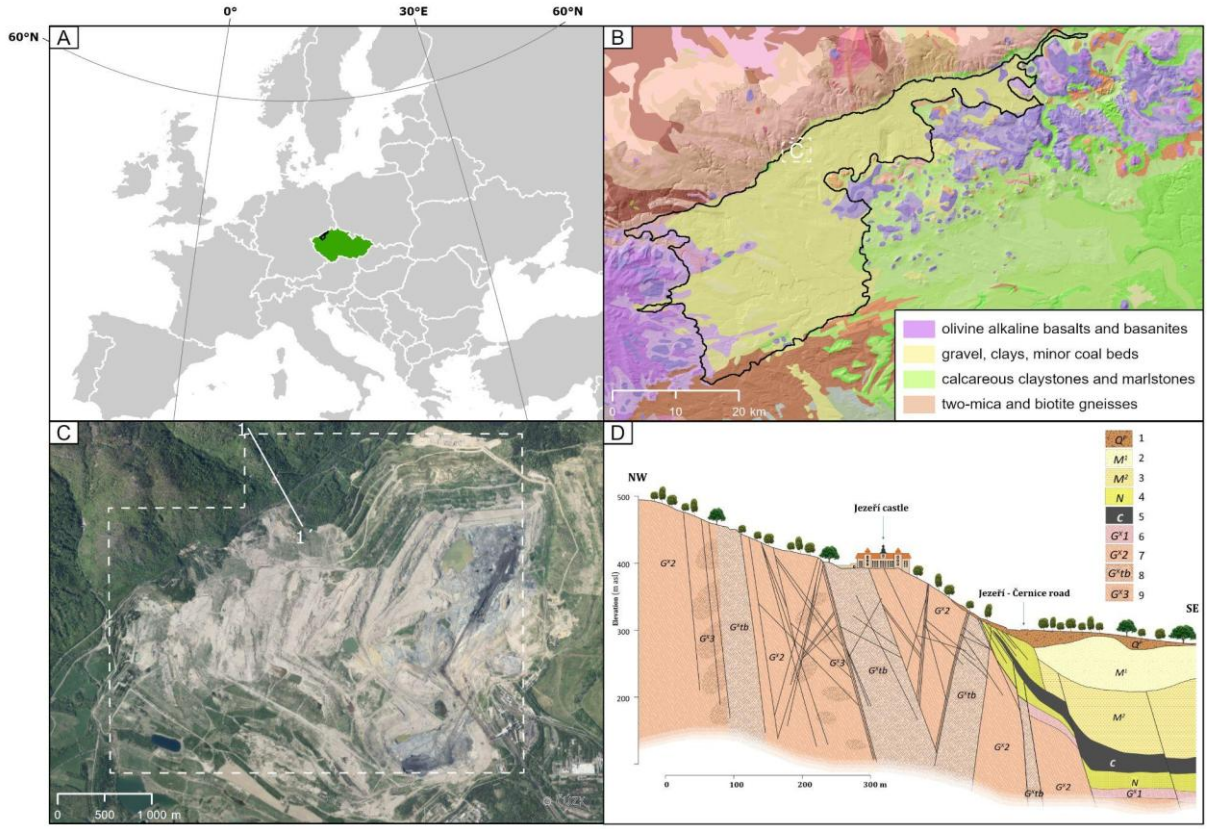

Fig. 1. Study area location map with: A Czechia, B geological map with boundaries of the Most basin, C study area, D geological cross-section from the study area: 1 – loamy to rocky colluvium and sandy proluvial gravels with boulders of solid orthogneiss; 2 – soft Miocene clays, usually disintegrating into small shards; 3 – stiff Miocene kaolinitic-illitic clays, horizontally bedded with indistinct tectonic disturbances; 4 – littoral and shoal Neogene sediments of medium to coarse-grained sandstones with a kaolinic binder; 5 – coal without (or only with thin) clay bands, at the basin's edge passing into carbonaceous siltstone; 6 – crystalline rocks, strongly weathered especially by kaolinisation; 7 – solid leaf-gneiss, foliation with an inclination of 40–60° into the basin; 8 – tectonic breccia chemically altered in the wide zones of a steep inclination, usually cemented gneiss, kaolinised debris, mostly without water; 9 – loosened solid gneiss with strong groundwater inflow, irregular occurrence of crushed zones (modified after: Mühldorf 1981)

Another major predisposition for landslides is the presence of underground water, which enters the site in two forms. The first in-flow type brings water from the crystalline slopes above the Most Basin outcrops. This type shows a direct dependence on atmospheric precipitation and causes interannual water-table fluctuations of up to 1m. The second type of inflow is represented by the permanent inflow of crystalline deep fracture-system groundwater. This system is characterised by constancy without seasonal fluctuations (Žižka & Halíř, 2010).
The anthropogenic terrain alteration can be dated to the 19th Century, but it has accelerated since the 1940s. Since the 1970s, the foothills of the Ore Mountains have been fundamentally transformed by open-cast brown coal mining and related terrain alteration for mining operations. Mining has lightened the base of the slope and loosened the crystalline rock outcrops. This combination causes some of the most extensive mass movements in the country Table 1. Landslides and accelerated sheet and gully erosion pose a key hazard for mining operations and future reclamation efforts.

Tab. 1. Overview of the most relevant mapped recent landslides

Year	Volume [mil. m^3]	Area [ha]	Depth [m]	Brief description and references
1983	6−8	N/A	58−65	This landslide, compared to the average in the Czech Republic, is sliding along a composite shear plane at the interface between Tertiary and Quaternary soils. The main scarp reached up to 510 m. The upper part had the character of a block movement with rotational slumping, down the slope, the sliding already continued up to the inner dump of the open-pit mine. References: Rybář (1996), Valeš (1998), Rybář (2006), Burda & Kycl (2023)
1984	N/A	22−24	60?	Gradual development of the surface has preceded the formation of the landslide. Sliding was reactivated in January 2011 on a larger scale with three earthflows (300–600m long) activated, and a complex landslide formed (length of 700m, width of 320m). The slightly curved main scarp is up to 80 m high and partly follows a weakened, tectonically predisposed zone in the Krušné hory slope. In the lower part, this landslide exceeds 1km in width. The thickness is estimated to be up to 60 m. References: Rybář (1996), Marek (2006), Burda & Kycl (2023)
2005	3−7	22,6	14,5−27	Deep-seated frontal landslide was gradually initiated in 2003 and 2004, when the first signs of failure of the service shaft (No. VI) reinforcement were observed. Cracking and breaking of the reinforcement were documented at a depth of approximately 27 m. On 19 June 2005, a block sliding of between 2 and 25 m occurred. The slide was subsequently rehabilitated. References: Rybář & Novotný (2005), Marek (2006), Burda & Vilímek (2010)
2011	1,7−3,9	21	15	Complex landslide with a total length of almost 1km and a maximal width of 340m. The displacement of the masses transported by slope movements was between 17 and 27 m in the upper part. Two partial earthflows formed in the landslide, with a velocity of movement significantly higher than that of the landslide. These ground currents were active for a longer period of time and led to the transport of masses from the displacement areas to the inner dump of the open-pit mine. References: Burda et al. (2011), Burda et al. (2013)
2013	15−20	51,3	26−39	A landslide with a complex system of shear planes has been active since June 2007, when the first tension crack was detected. Since 2007/2008, a cyclic progression of movements has occurred. In 2012, a runout landslide occurred when soils were transported from the source area to the bottom of the open-pit, where they covered the coal seam. In 2013, the entire slope collapsed, with the landslide transitioning into earthflows and mudflows that flowed to the bottom of the open-pit. The triggering factor was rainfall. The slide was subsequently remediated. References: Burda (2014), Burda & Kycl (2023)

Data and Methods

Research concept

A bivariate statistical analysis (van Westen et al., 1997; Meten et al., 2015; Dahal, 2017; Kadirhodjaev, 2018) based on frequencies of causal conditions and triggers and landslide inventories (weights of evidence) was used to create a landslide susceptibility model for the study area. The method is especially suitable for its possibility of reproducing the procedure in other sites where the closure of mines and future reclamation and reuse plans will be considered. The methodology proposed by this work comprises the steps shown in Fig. 2 and further explained in the following sections.

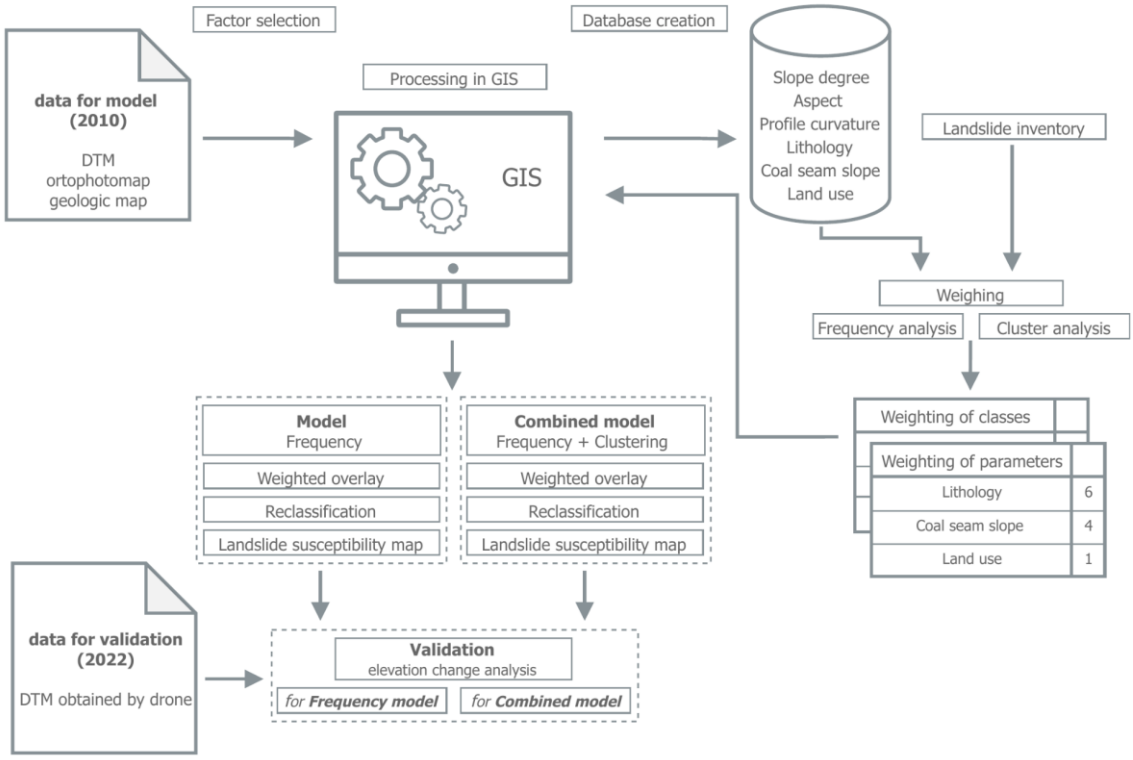

Fig. 2. Workflow of the susceptibility assessment and its validation

Data

Elevation data

The datasets for landslide inventories were based on official public data and our own surveys. In the first step, data from the digital elevation model DMR 5G, an official data source for Czechia from 2010 (ČUZK 2016), were processed. The DMR 5G data has a mean height error of 0.18m in exposed terrain and 0.3m in forested terrain. We consider such accuracy to be sufficient for the needs of the study area, where height changes over time can reach up to 50m. Based on these data, an elevation raster (1m/pixel resolution) was created to derive parametric maps (slope, aspect, and vertical curvature) in ESRI ArcGIS Pro.

Contributing factors

Established environmental parameters - slope, slope orientation, curvature, coal seam slope, geological conditions, and vegetation cover — were pivotal in selecting the bivariate analysis for landslide susceptibility in the study (Segoni et al., 2020; Dahal, 2017; Kadirhodjaev et al., 2018).

(a) Slope is a fundamental parameter due to its correlation with gravitational effect (Kadirhodjaev et al., 2018; Segoni et al., 2020). Slope orientation correlates with solar radiation and water infiltration, which in turn affect soil moisture, weathering cycles, and vegetation cover – all of which influence slope stability. Curvature, on the other hand, indicates areas where tension or compression forces may be dominant, impacting landslide susceptibility. Slope, slope orientation, and slope curvature were derived from the digital elevation data.

(b) Geological conditions provide insights into the underlying rock types, fault lines, and geological structures that can predispose landslides (Segoni et al. 2020; Dahal 2017). The interface between overlying sediments and the coal seam represents one of the key geotechnical interfaces (Reanud et al., 2022). Hence, the inclination of the seam is one of the determinants of slope stability. The inclination of the coal seam also translates into the inclination of all overlying layers and other geotechnical interfaces in outcrop areas (typically at the foot of mountains - see Fig. 1D). It is, therefore, a suitable indicator of deteriorated stability conditions. The geological map and the map of coal seam slope were derived from detailed geotechnical sections (Valvoda et al., 2020).

(c) Finally, vegetation cover plays a significant role in landslide susceptibility as it can affect soil cohesion and infiltration, impacting slope stability (Kalsnes & Capobianco, 2022). Areas with sparse vegetation cover are often more prone to landslides, especially in regions with steep slopes and high rainfall. The vegetation map was derived from an orthophoto map (1m/pixel) taken in 2010.

The classes for all continuous parameters were established as manual intervals on a standardised scale (1–5). The manual intervals have been set according to the classes used in the literature (Reichenbach et al., 2018;

Segoni et al., 2020) and reflect the empirical relations between the parameters, terrain stability, and landslide occurrence.

For the validation dataset, the UAV survey (Phantom 4 RTK) was conducted in the spring of 2022. A total of 907 images were captured with 70% horizontal overlap and 80% vertical overlap. The ground resolution was 0.0360m. The generated digital elevation model had a grid resolution of 0.3m and an average point density of 114.15 points/m². The elevation raster used for validation analysis had a 1m/pixel resolution for optimal comparison with the 2010 raster. Known coordinates of points from the monitoring network or hydrological boreholes were used as ground control points (GCPs).

Landslide inventory

An essential prerequisite for landslide susceptibility maps is a landslide inventory. We used a combination of DTM, orthophoto maps, and field surveys. To reduce the subjectivity of landslide inventory (see Carrara et al., 1995), the following set of criteria was defined to determine which landslide types would be inventoried (see Fig. 3 for the method and Fig. 4 for the resulting inventory): (i) Landslides A with an area larger than 1000m² or cracks B with a continuous character, longer than 100m, were inventoried. (ii) Smaller landslides are frequently linked to mining stages (i.e., step-like profiles). Where local landslides connect to form a continual topography of stage C, the whole mining stage has been mapped as a landslide. On the other hand, where local landslides interrupt the continuity of mining stages and where boundaries of a compact instability could be detected, they were mapped as individual landslides D.

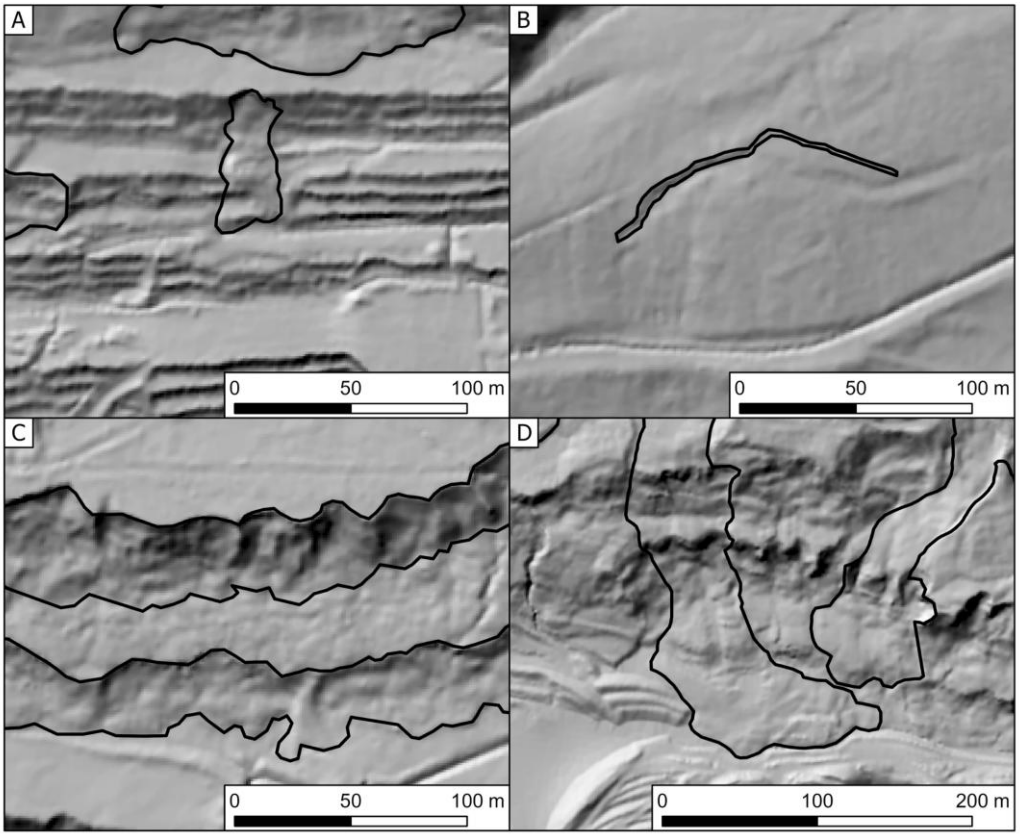

Fig. 3 Landslide types delineated according to inventory criteria

Methods

Weighting and susceptibility models

The process of assigning weights to classes within contributing factors (primary weight) and to individual parametric maps of contributing factors (secondary weight) was based on a combination of two different approaches. First, a rather conventional frequency analysis (Yalcin, 2008; Dahal, 2017; Buša et al., 2019; Hodasová & Bednarik, 2021) was used to identify the occurrence of parameter classes within the landslides and across the whole area. In landslide susceptibility models, frequency analysis assumes that variations in landslide susceptibility result from the interplay of the differential contributions of individual factors to landsliding. The analysis is therefore based on calculating the proportions of landslide areas pertaining to individual classes of contributing factors. Primary weights for contributing factors are assigned as the proportion between the area

occupied by landslides in a particular parameter class and the total area of that class. In this step, each class was given its own weights. The resulting weights for all parameter classes were summed and divided by the number of classes to obtain the secondary weight for each parametric map.

Since the frequency analysis does not account for the differential spatial distribution of parameter classes, we also opted for a cluster analysis using the Average Nearest Neighbor tool in ESRI ArcGIS Pro. This method allows us to spatially aggregate the parameter classes within the landslides and in the whole area. This approach is based on comparing how classes within the parameters form clusters within the landslide and across the whole area. If the values of a selected class form clusters within landslides and are scattered across the whole area, this class is expected to contribute significantly to the area's landslide susceptibility. The nearest neighbour index is expressed as a ratio of the observed mean distance to the expected mean distance. The expected distance is the mean distance between neighbours in a hypothetical random distribution[1]. If the index is less than 1, the sample exhibits clustering; on the other hand, if the index is greater than 1, the trend is toward dispersion or competition (ESRI, 2022).

Using the weighted overlay tool, two landslide susceptibility models were created in ESRI ArcGIS Pro software: (i) Frequency model incorporating only the results derived from frequency analysis, and (ii) Combined model integrating (using the multiply function) results from both the Frequency and the Cluster analysis. The model results were reclassified into four susceptibility classes (low, medium, high, and very high) so that the number of pixels in each class for the two models was comparable.

Model validation

According to Reichenbach et al. (2018), validation is a key component for obtaining a higher Susceptibility Quality Level (SQL) for landslide susceptibility maps. Several different accuracy validation methods are used in statistics for prediction models (probabilities) in the assessment or analysis of disasters. Their use depends on the specific local conditions, available technology, and data. Conventional methods include, for example, an Area under the Curve (AUC) analysis involving a success rate curve and a predicted curve, or the analysis of the so-called ROC (Receiver Operating Characteristic) curve (Silalahi et al., 2019; Ujjwal et al., 2020). In the present research, we opted for SQL4, which is based on estimates of model-prediction performance derived from data distinct from those used to prepare the susceptibility model itself (Reichenbach et al., 2018). The approach was based on comparing cumulative surface deformations, calculated as the difference between the 2010 data used for a landslide susceptibility model and the 2022 data obtained by UAV (Section 3.1). The method compares the model predictions for individual susceptibility classes with the actual changes in the terrain that may be caused by landslides and identifies other possible interventions causing the changes. The validation has been conducted in a validation area mostly affected by landslides over the last decade (Fig. 7). The area was chosen to cover the highest relative extent and diversity of landslides, the occurrence of new landslides, and with remediation and reclamation limited mainly to the foot-slopes, thus preventing too extensive influence of human modifications on the results. The validation was based on analysis of height differences of the two terrain datasets (2010 and 2022) for the entire area, and also separately for the areas within and outside of the landslide.

Results

Landslide inventory

The landslide inventory for the study area in 2010 is shown in Fig. 4. Overall, 38 landslides were mapped according to the criteria described in the methodology. Their average area is ca. 24,653 m^2. The most extensive landslide with an area of 82,421 m^2 was recorded in the W part of the site, where other large landslides were also located. The SW-facing slopes have more complex geological conditions than the SE-facing slopes, which are predominantly composed of clay, resulting in higher typological homogeneity of landslides. In the SW part, there are extensive deep landslides (some of them deep-seated), which often turn into earth flows in distal zones. These landslides cross several overburden benches, and their average area in this part is about 32,100 m^2. The SE part differs, with landslides occurring within one or, at most, two overburdened benches. The average area of these landslides is almost half that of the W part (16,800 m^2). To validate the model, a comparative inventory was created based on the 2022 data. The validation inventory identified a total of six new landslides with an area of 261,150 m^2.

[1] In ESRI ArcGIS Average Nearest Neighbor tool, the hypothetical random distribution is based on a square root of number of features divided by the area of a minimum enclosing rectangle around all features.

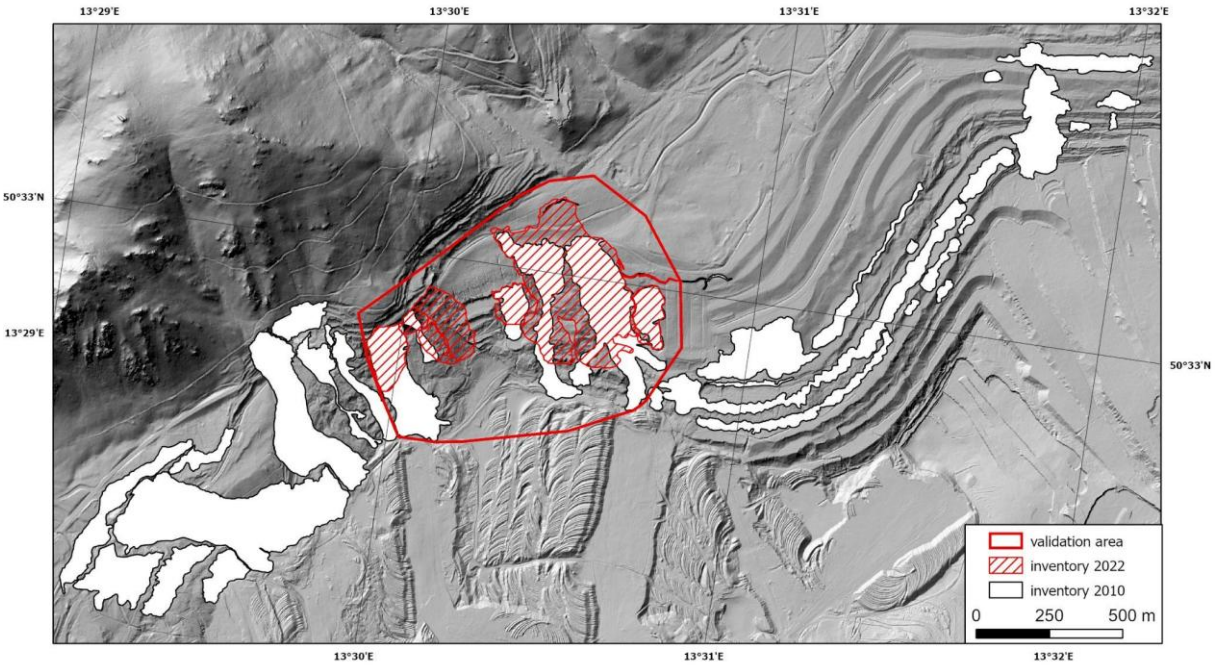

Fig. 4 Landslide inventory map from 2010 and 2022

Landslide susceptibility models

Results of weighting classes of input environmental parameters

In this section, we present the results of the frequency and cluster analysis. We comment mainly on the most divergent results and the results that we consider to be anomalies. Generally, steeper slopes are more prone to slope movement. In the study area, this is also evident in the frequency analysis, where the 50 - 90° slope class received the highest weight. To the contrary, the 0 - 5° class covers approximately 42% of the entire area, yet its presence within landslides is very low (8%), and was assigned the lowest weight accordingly. Different results were obtained using the nearest neighbour index. Here, the clustering was very high within landslides for the 50–90° slope class, but significant clustering was also observed in the entire area, denoting that slope inclination itself does not represent a decisive condition for landsliding.

Moving to lithology, the claystones have the highest representation in the study area, except in the area marked as mined-out, and they are present in 66% of the landslides; therefore, they have the highest weight. The clustering results are quite interesting: the highest weight was obtained by crystalline rock and regelation clay, to which a number of scarp zones of landslides or rockfalls are tied, which then transition into landslides. There was a subjective intervention in the procedure for assigning weights to each class for the mining area and Miocene sands, as they are not represented in the landslides.

Landslide susceptibility

Figure 5 shows susceptibility maps generated using the Frequency and Combined models. Fig. 5A shows the distribution of susceptibility classes in both models. To ensure consistency in the model evaluation, all susceptibility classes were evaluated based on their proportions of the total study area and their overlap with mapped landslides. The low-susceptibility class covers a significant portion of the study area but shows minimal overlap with mapped landslides (Fig. 5B). The Frequency model predicted inventoried landslides well, with 63% of the landslide-affected areas classified as high-susceptibility. In contrast, the Combined model provided a stronger representation of the very high susceptibility class, which accounted for 50% of the landslide-affected areas. For the area outside of inventoried landslides (Fig. 5C), high and very high susceptibility classes remain limited, covering only a small portion of the study area. Finally, Fig. 5D compares model results with 2022 landslide inventories. The results align with those in Fig. 5B, while also incorporating the low susceptibility class. The Combined model performed better in predicting landslides within the very high susceptibility class. This trend is even more evident in Fig. 7, where the scarp zones of all newly developed landslides fall within the high susceptibility class.

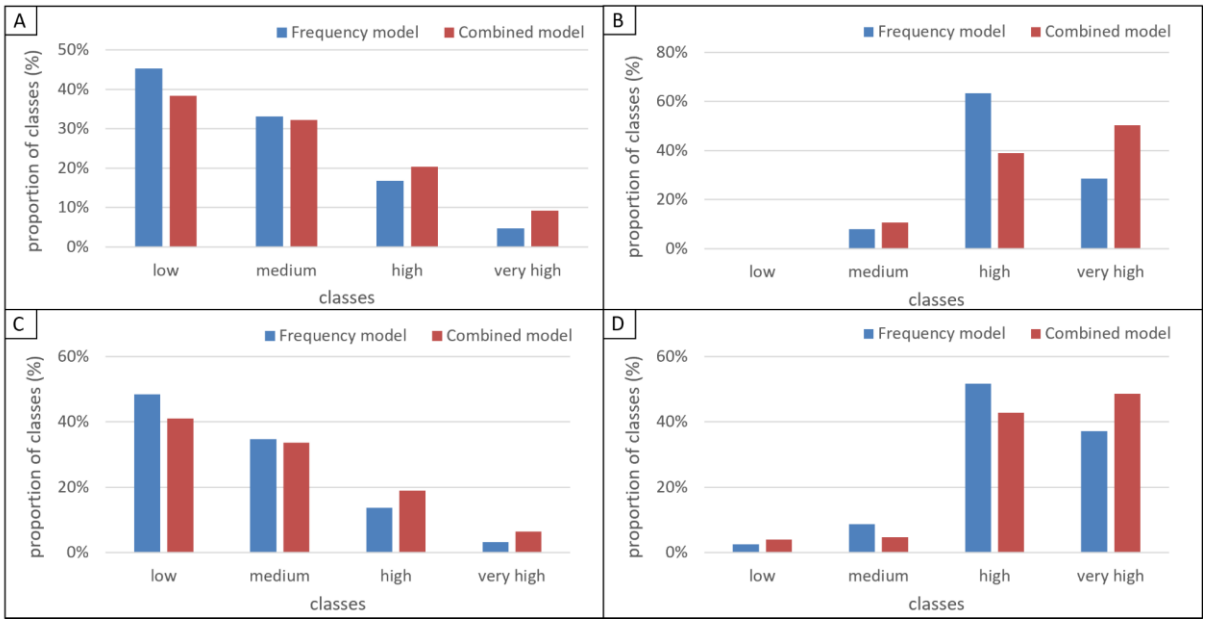

Fig. 5 (A) Percentage distribution of susceptibility classes in both models, (B) Comparison of model results with landslide inventories from 2010, (C) Representation of susceptibility classes outside of landslides, (D) Comparison of model results with landslide inventories from 2022

ROC (Receiver Operating Characteristic) curves were used to evaluate the performance of landslide susceptibility models. These curves show the relationship between the false positive rate (FPR) and the true positive rate (TPR) across different threshold values. The modeled susceptibility grids (Frequency and Combined models) were converted into probability maps based on predefined classes. For each pixel, the probability of a landslide occurring was assigned, and at the same time, the actual value was extracted from the binary map of actual landslides (1 = landslide, 0 = stable area).

Using this data, ROC curves and corresponding AUC (Area Under Curve) values were calculated, which quantitatively express the model's ability to distinguish between stable and landslide-prone areas. The analysis was performed separately for the entire modeled area and for the validation area.

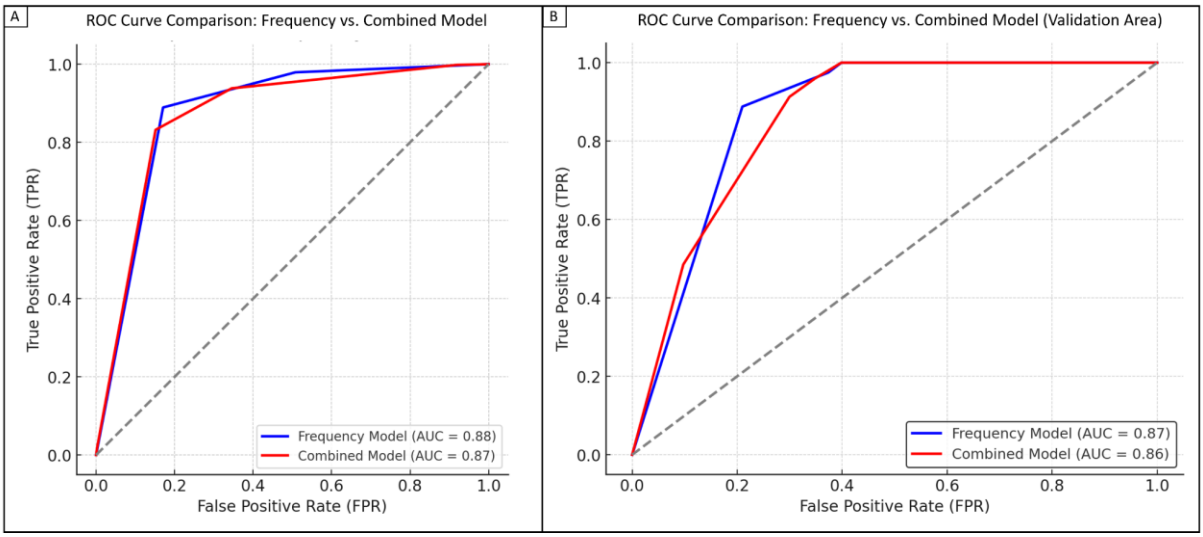

Fig. 6 ROC curve for the Frequency and Combined models: (A) 2010 training model, (B) 2022 validation model

ROC (Receiver Operating Characteristic) curves for both the 2010 and 2022 models (Fig. 6) show that both models have very similar ability to distinguish between landslide-susceptible and stable areas. The Frequency model performs slightly better, but the difference in AUC (Area Under the Curve) is small (0.88 vs. 0.87). The Combined model identifies more stable areas as susceptible and has a higher false positive rate (Frequency model: 0.45 False positives; Combined model: 0.6 False positives). In the validation area, the Frequency model (AUC = 0.87) again performed slightly better than the Combined model (AUC = 0.86). However, the Combined model had a lower false positive rate (Frequency model: 0.37 False positives; Combined model: 0.29 False positives).

Model validation

The predictive efficacy of the landslide susceptibility models was tested in the validation area (see Method, which was used to create a digital terrain model in 2022). The area has been partly anthropogenically influenced over the studied timeframe, but the extent of these terrain alterations can be strictly delimited compared to other parts of the mine. The other parts of the mine's side slopes have undergone remediation over time.

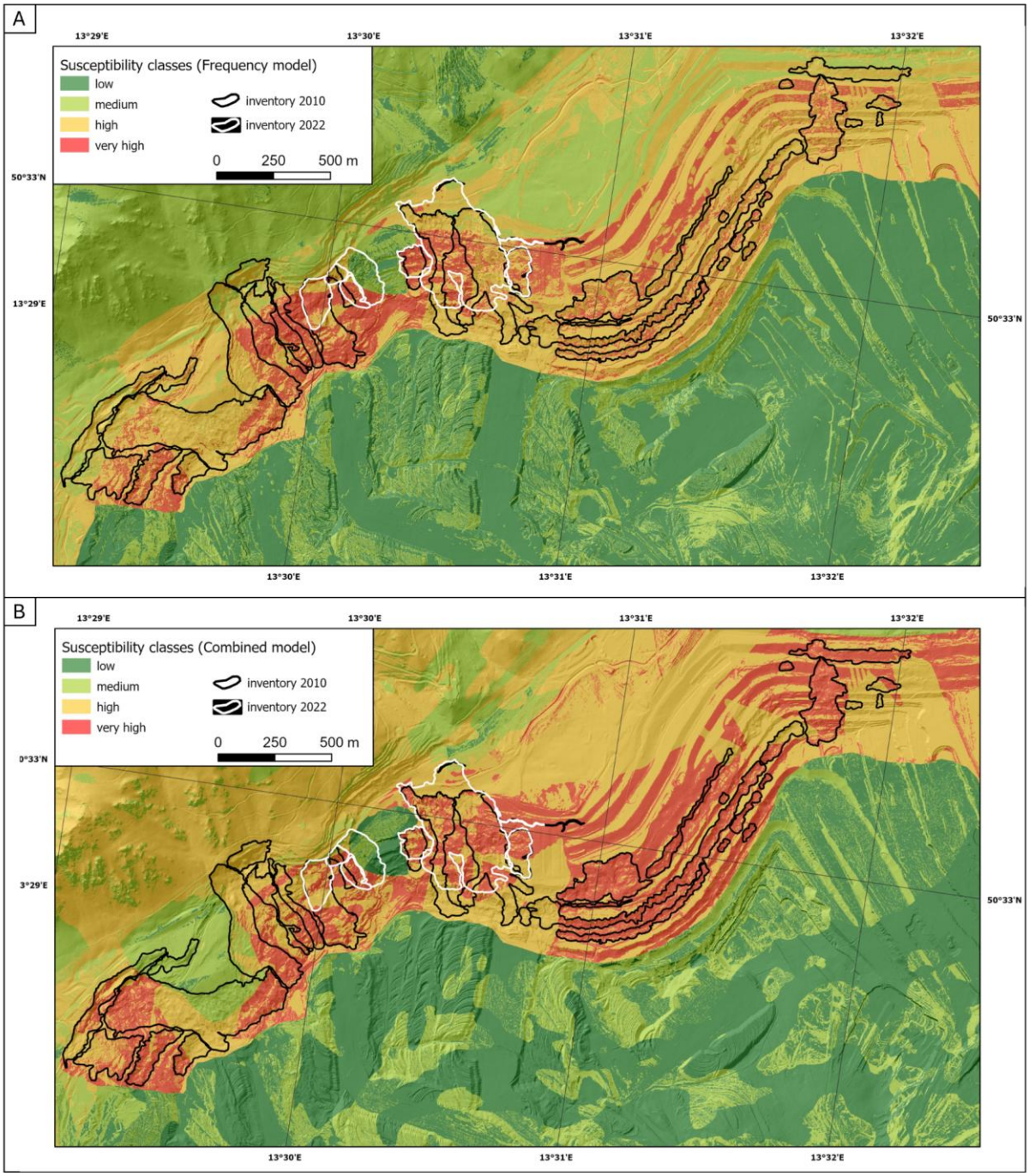

Fig. 7 Landslide susceptibility map for (A) Frequency model and (B) Combined model

Using the two landslide inventories, we compared in detail the changes that have occurred and identified their causes over a relatively long period, 12 years. Significant changes in mass balance have been identified by subtracting the raster with the elevations from 2022 from 2010 (Fig. 8). Based on the elevation changes, the contours of the landslides are clearly identifiable, and there is also a distinct division into scarp areas in the upper part of the slope (decrease in altitude) and accumulation areas in the lower part (increase in altitude). In the scarp area of the largest landslide, the decrease in altitude reaches up to 19.8m (Fig. 8A). In the west, we also observe a decrease of about 15m (Fig. 8B) caused by rockfall from crystalline outcrops, which then turned into a landslide.

On the other hand, the accumulation part is characterised by a terrain rise of 10 - 20m (Fig. 8C). In the lower part of the slope, there was anthropogenic intervention; therefore, this area was delimited in the map. The changes in this part are associated with the filling of the internal dump, hence the anthropogenically-induced positive mass balance of up to 49.3m (Fig. 8D).

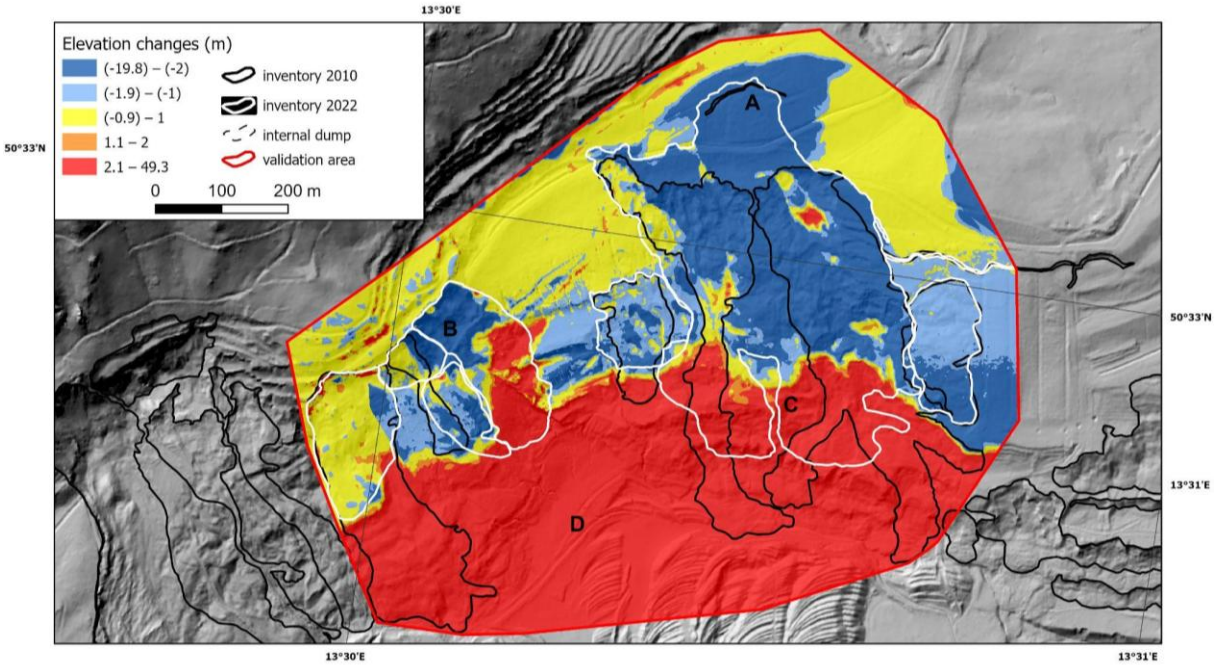

Fig. 8 Map of elevation changes between 2010 and 2022

By comparing terrain elevation changes (Fig. 8) with landslide susceptibility maps for both models, the predictive capability of the individual susceptibility classes was assessed. The inner dump area was excluded from the validation because it was the most anthropogenically influenced, which would have biased the results. The Frequency model results for the entire validation area (Fig. 9A) indicate only minor elevation changes in the low- and medium-susceptibility classes. Q1 and Q3 indicate the 25th and 75th percentiles of terrain elevation change, respectively. Negative values represent terrain lowering, while positive values reflect accumulation or uplift. The interquartile range (Q3 – Q1) further illustrates the variability of terrain response within each susceptibility class. In the high susceptibility class, higher elevation changes are observed, which rather represent terrain lowering (Q1) = -4.14m, (Q3) = 0.09m. In the very high susceptibility class, the changes are slightly lower (Q1) = -2.26m (Q3) = 1.06m. For the Combined model (Fig. 9B), the results are similar, except for the medium susceptible class. Significant terrain lowering has been assigned to this class (Q1) = -3.34m, (Q3) = 0.17m.

Outside inventoried landslides, the Frequency model (Fig. 9C) exhibits relatively high terrain changes in the highest susceptibility class (Q1) = -1.73 m and (Q3) = 4.55m. The latter represents a positive terrain balance, likely related to the remediation of the lower part of the original landslide in the western part of the area, where a service road was also built. In contrast, the Combined model (Fig. 9C) indicates that apart from mapped landslides, there have been no significant terrain changes in any of the susceptibility classes.

For the main scarp, the Frequency model (Fig. 9D) shows that the medium susceptible class primarily represents lowering (Q1) = -6.96m, (Q3) = -2.78m, yet the high susceptibility class predicts the scarp zones most accurately (Q1) = -8.34m, (Q3) = -1.08m. The Combined model (Fig. 9E) also primarily indicates a lowering in the main scarp. However, these are slightly higher across all susceptibility classes than in the Frequency model. Nevertheless, the medium susceptibility class (Q1) = -7.63 m, (Q3) = -0.49 m, and the high susceptibility class (Q1) = -7.31 m, (Q3) = -1.02 m were slightly higher.

For the main body (accumulation segment), the Frequency model (Fig. 9G) results for the landslide accumulation zone show significant terrain uplift in the medium, high, and very high susceptibility classes. There were almost no changes in the low susceptibility class. In the Combined model (Fig. 9H), a significant difference in the low-susceptibility class was observed, with relatively high terrain uplift (Q1) = 0.92m and (Q3) = 11.13m. Predicting accumulation zones is more complex than scarp zones, since multiple expansions may occur due to mudflows in complex landslides. The results may therefore have higher variability.

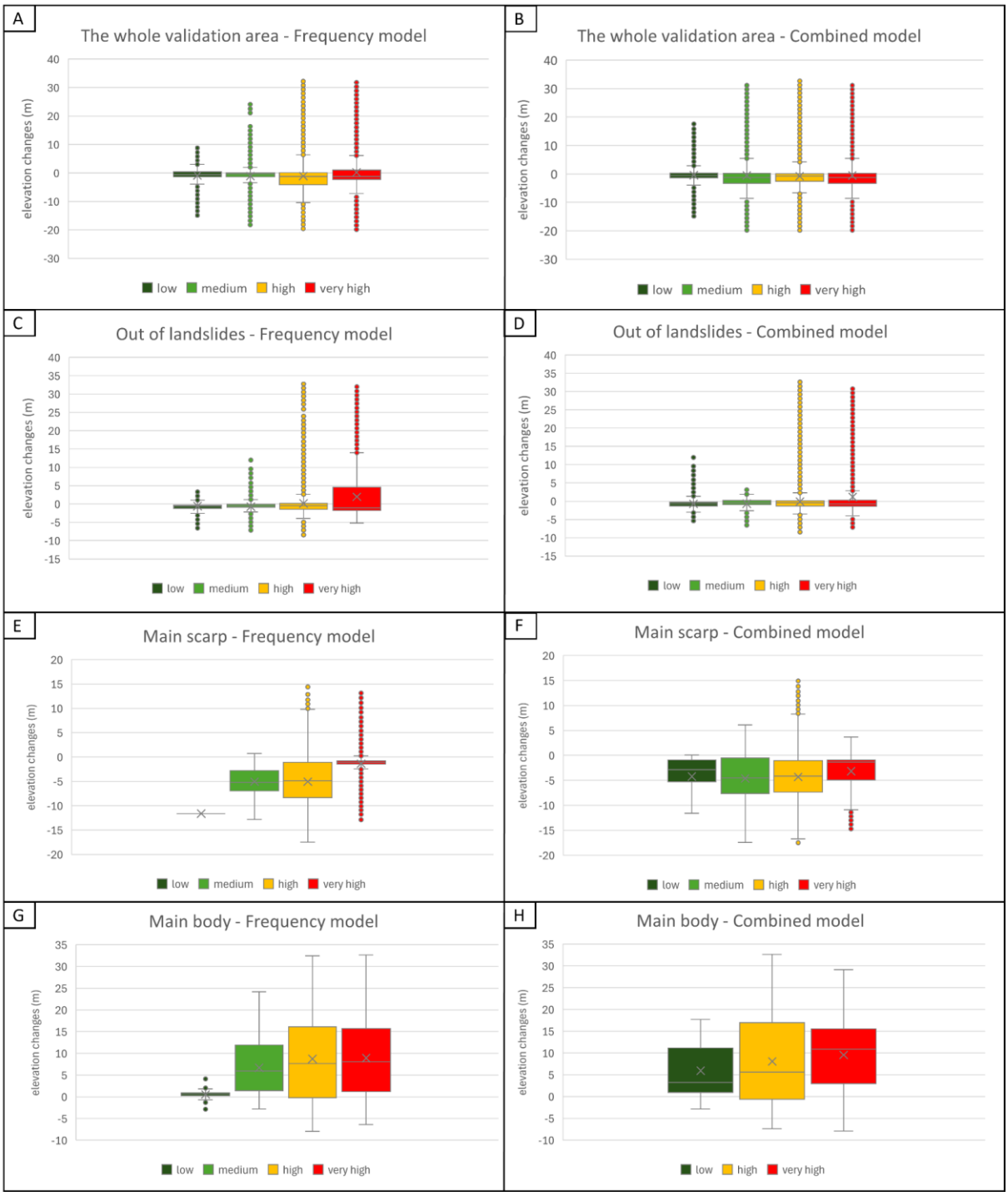

Fig. 9 Validation of the predictive ability of a landslide susceptibility model by boxplot: (A) Frequency model and (B) Combined model for the whole validation area, (C) Frequency model and (D) Combined model for the part out of slope deformation, (E) Frequency model and (F) Combined model for the scarp zone, and (G) Frequency model and (H) Combined model for accumulation zones.

Finally, we performed a statistical analysis of the differences between the two models to determine whether the differences among susceptibility classes are significant. As the datasets met the criteria for a parametric test, one-way ANOVA was used to assess differences, and post hoc Tukey's HSD test was applied to detect specific patterns of differences among susceptibility classes (Table 2). Both models displayed statistically highly significant differences among the susceptibility classes ($p < 0.000$) in the whole area, outside inventoried landslides, in the main scarp, and in the main landslide body. The post-hoc test showed that statistically significant differences in terrain changes occur among the susceptibility classes, with non-significant results observed mainly in pairwise comparisons between the low and medium susceptibility classes. The weakest results were obtained for the main scarp zones, which are represented by smaller areas that are subject to inventorying bias due to multiple extensions and the occurrence of cracks.

Tab. 2 Statistical evaluation of the ability of models to distinguish between the individual susceptibility classes

		Low (L)		Medium (M)		High (H)		Very High (VH)		ANOVA (F value)	Tukey's HSD Test 95% C.I.			
		Mean	SD	Mean	SD	Mean	SD	Mean	SD		*p<0.000*	*p<0.001*	*p<0.01*	*p<0.05*
Whole area	Model 1	-0,90	3,09	-1,11	3,01	-1,07	6,96	0,21	7,16	1470	*all, except M-H*			
	Model 2	-0,44	3,34	-0,54	6,98	-0,82	6,29	-0,54	6,98	98,64	*L-H, M-H, H-VH*			*L-M, L-VH*
Outside landslides	Model 1	-0,56	1,00	-0,74	1,35	0,18	4,13	1,96	5,86	5765	*all*			
	Model 2	-0,73	1,14	-0,69	1,45	-0,10	3,50	1,16	5,15	2839	*all, except L-M*			
Main scarp	Model 1	-4,22	4,10	-4,60	4,52	-4,32	4,14	-3,17	3,62	133,3	*M-VH, H-VH*		*M-H*	
	Model 2	-11,62	N/A	-5,05	2,78	-5,04	4,26	-1,36	2,56	1370	*M-VH, H-VH*			*L-VH*
Main body	Model 1	0,57	0,81	6,68	5,83	8,72	9,11	8,92	8,01	81,68	*all, except H-VH*			*H-VH*
	Model 2	5,95	5,66	N/A	N/A	8,06	9,72	9,57	7,30	286,1	*all*			

Note: All mean and SD values are given in [m]. Differences in all models are significant at p<0.000

Discussion

Statistical analysis is a widely used approach in landslide susceptibility modeling (e.g., Meten et al., 2015; Dahal, 2017; Kadirhodjaev et al., 2018; Buša, 2019; Al Heib et al., 2023). However, its application in brown coal open-cast mines and reclamation planning remains largely unexplored. This study develops and validates two statistical models for landslide susceptibility in a small area of an open-cast brown coal mine in northwest Czechia (Central Europe).

The models are based on a 2010 landslide inventory and a series of parametric maps of geo-environmental conditions. Susceptibility maps and classification were derived using statistical processing through Frequency Analysis and a Combined Approach integrating Frequency and Cluster Analyses in GIS. Model validation was performed using a repeated landslide inventory from 2022 and terrain deformation data obtained via UAV surveys in the same year. Overall, both models demonstrated a good fit with the observed landslides.

The predictive performance of the models was assessed in a validation area. The Frequency Model was particularly effective at predicting elevation changes (i.e., landslide-induced deformations) in the high-susceptibility class, accurately delineating scarp zones. The very high susceptibility class also captured middle slope sections and landslide accumulation zones. In middle-slope areas, this pattern is attributed to retrogressive failure processes, including scarp development and tension-crack formation within the main landslide body. Additionally, new shear zones were observed at higher elevations, possibly related to terrain irregularities, although further investigation is needed to clarify this relationship. In the accumulation zones, high susceptibility values were observed in steep landslide toes, which are prone to further displacement and spreading.

The Combined model produced distinct results, with the clustering procedure yielding the most accurate prediction of elevation changes across the entire study area, particularly in the scarp zone within the medium susceptibility class. Beyond evaluating the spatial alignment between susceptibility classes and the validation landslide inventory, it is also crucial to assess the predictive capabilities of individual susceptibility classes. The validation process revealed significant (ANOVA; $p < 0.000$) differences in predictive performance across susceptibility classes in both models, indicating a high ability to distinguish them. A post hoc Tukey's HSD test indicated that the non-significant differences were primarily observed between the low and medium susceptibility classes. This outcome likely results from the use of equal intervals in class delineation. Consequently, the low- and medium-susceptibility classes encompassed areas of internal dump deposits, where anthropogenic mass accumulation (up to 49.3 m) may obscure or blend with deformations induced by earthflows moving downslope from landslides. Based on these validation results (SQL4; Reichenbach et al., 2018), we conclude that the models are generally effective at predicting landslide occurrences in the study area. However, they also highlight key challenges that need to be addressed in future model development.

Specific requirements for data accuracy and interpretation in reclamation practices necessitate the adoption of less conventional weighting approaches, such as a combination of Frequency and Cluster analysis, or validation methods based on terrain topography changes (e.g., the validation of DTM in this study). A key distinction from other studies is the need for highly detailed DTM data and other environmental factors influencing landslides, which may vary significantly between mining and non-mining sites. Furthermore, mining sites often exhibit greater variability in these factors due to ongoing or even receding mining activities. This necessitates temporal

deaggregation of the data to clearly distinguish pre-landslide and post-landslide conditions. However, this process poses considerable challenges, as past landslides may exist at different stages of development, potentially triggering new landslides or reactivating existing ones in varying ways.

In this paper, we utilized a set of parameters commonly employed in landslide susceptibility studies, but their accuracy and associated uncertainties require further discussion. Parameters derived from DTM-based morphology, such as slope, aspect, and surface curvature, are generally considered precise (see Data section). However, these parameters may introduce uncertainties into susceptibility models, as they reflect terrain conditions that have already been altered by past landslides. The vegetation parameter is also subject to uncertainty due to potential misclassification of certain features during automatic and supervised classification of aerial imagery—for instance, smaller water bodies may be misidentified. Additionally, the slope of the coal seam is a critical parameter in mining areas. Other potential parameters relevant to mining regions, such as historical underground mining structures, were considered but ultimately not incorporated due to data limitations. Lithological conditions present another challenge. Publicly available geological maps often lack sufficient detail, and open-cast mining areas are frequently depicted as "white spots", indicating missing data. In contrast, mining companies maintain detailed geological surveys of their sites, typically in the form of geotechnical sections or borehole records. The process of converting this data into a spatially explicit geological map may introduce minor inaccuracies. Nevertheless, incorporating this parameter was crucial (e.g., Segoni et al., 2020), as geological conditions play a fundamental role in landslide mechanisms. Another source of uncertainty specific to mining areas is the reliability of landslide inventories. Continuous terrain modifications, characteristic of mining sites, can influence both the dynamics and complexity of landslides. Consequently, the assumption of stationarity—a key premise in statistical landslide susceptibility models—is not fully applicable in these environments.

To minimize uncertainties in data analysis, we implemented a weighting procedure that advances objective weighting rather than heuristic approaches, in which weights are subjectively assigned based on expert judgment. Our method derives weights by aggregating parameter values for inventoried landslides, using a combination of Frequency Analysis and Cluster Analysis. Validation using ROC curves and independent datasets demonstrated that this approach is reliable when compared to conventional methods. However, certain weight assignments remain open to discussion. Weighting each parameter class according to Frequency Analysis yielded expected results, aligning with findings from other landslide susceptibility studies. In contrast, Cluster Analysis produced some atypical results, particularly concerning slope and vegetation parameters. In these cases, the assigned weights contradict established landslide mechanisms documented in the literature (e.g., Kalsnes & Capobianco, 2022). For instance, steep-slope areas were predominantly clustered in lower-susceptibility classes. This anomaly may be attributed to the presence of minor scarps and tension cracks, which are distinct landforms that become emphasized through pixel clustering in raster-based analysis. Conversely, in some instances, Cluster Analysis outperformed Frequency Analysis. For example, it assigned the second-highest weight to the geological condition parameter within the clay regulatory zone. This result is particularly relevant, as shear surfaces of certain deep-seated landslides are associated with this zone. These findings provide valuable insights into the dependence of detached landslide surfaces on lithological conditions.

These results indicate that while cluster analysis offers valuable insights, its outcomes for certain parameters—such as slope and vegetation—should be interpreted with caution. The observed discrepancies suggest that further refinement or the integration of complementary methods may be necessary to improve the reliability of parameter weighting. Additionally, expert validation is crucial for assessing the relevance of the obtained results to landslide mechanisms. In this regard, the findings highlight that the two models serve different applications and may be more suitable for distinct parameter types. The Frequency model demonstrated higher accuracy in delineating landslide boundaries and scarp zones, making it particularly effective for assessing stable and unstable areas in regions already affected by landslides. Due to its precision, this model can be effectively used to monitor susceptible areas and conduct long-term observations of their development. Conversely, the Combined model identified a broader range of potentially susceptible areas, including locations where landslides have not yet been recorded but where geological and morphological conditions favor their occurrence. This approach is especially beneficial for spatial planning and proactive risk management, such as identifying areas unsuitable for construction or locations where slope stabilization measures should be implemented before future land use decisions. Typically, susceptibility models are applied at medium to small scales, such as at the regional or national level. However, with the inclusion of high-quality, more specific input data, these models have proven suitable and highly useful - particularly when presenting results to spatial planners and land development stakeholders who may lack specialized expertise in landslide-related issues.

Conclusions

Landslide susceptibility modelling has seen dynamic development, yet existing models have been scarcely validated in the context of open-cast brown coal mines. These mines are currently undergoing closure and reclamation, necessitating tailored approaches to address potential landslide hazards. In this paper, we developed

and validated two landslide susceptibility models for the open-cast brown coal mine in the Most Basin, NW Czech Republic (Europe), an area with a high landslide occurrence documented over the last decades and where reclamation efforts are now being considered. Our results can be summarized in three main recommendations for future research. First, while both the Frequency and Combined models successfully predicted landslides and classified susceptibility, they are suited to different purposes. Second, applying these models to open-cast brown coal mines requires including parameters that are typically absent in conventional landslide susceptibility models. In the future, geomechanical properties, penetration test results, or groundwater level heights could be incorporated into the modelling. Third, it is necessary to consider the specific terrain dynamics, triggering factors, failure types, and landsliding mechanisms in open-cast brown coal mines. Compared to other environments, this primarily includes continuous direct anthropogenic changes to slopes and internal dumps, which influence susceptibility parameters and landslide behaviour (e.g., retrogressive development, tension cracks). This requires the availability of time series for temporal data disaggregation. These recommendations highlight the international relevance of our study for brown coal mining sites undergoing closure and reclamation. The unique aspects of our susceptibility models present a challenge for future research to validate additional parameters specific to mining sites. Finally, a key challenge lies in effectively communicating and implementing susceptibility models in reclamation projects. This requires interdisciplinary collaboration with planners to co-develop landslide susceptibility models that are comprehensible and provide clear protocols for interpreting results and their uncertainties.

References

Al Heib, M., Varouchakis, E.A., Galetakis, M., Renaud, V., & Burda, J. (2023). A framework for assessing hazards related to pit lakes: application on European case studies. Environmental Earth Sciences, 82, 365. https://doi.org/10.1007/s12665-023-11045-4

Amirshenava, S. & Osanloo, M. (2018). Mine closure risk management: An integration of 3D risk model and MCDM techniques. Journal of Cleaner Production, 184, pp.389–401. https://doi.org/10.1016/j.jclepro.2018.01.186

Bárta, Z., Brus, Z., Hurník, S., Toběrná, V., & Tyrner, P. (1973). Příroda Mostecka. Ústí nad Labem: Severočeské nakladatelství.

Böhm, H, Boháč, A., Novotný, L., & Kurowska-Pysz, J. (2025) The impact of the dispute over the Turów Mine on Polish-Czech cross-border cooperation. GeoScape 19(1), pp.77–91. https://doi.org/10.2478/geosc-2025-0006

Braun, J. & Hánek, P. (2014). Geodetic monitoring methods of landslide-prone regions – application to Rabenov. AUC Geographica, 49(1), pp.5–19. https://doi.org/10.14712/23361980.2014.2

Burda, J. & Vilímek, V. (2010). The influence of climate effects and fluctuations in groundwater level on the stability of anthropogenic foothill slopes in the Krušné Hory Mountains, Czechia. Geografie, 115(4), pp.377–392. https://doi.org/10.37040/geografie2010115040377

Burda, J., Žížka, L., & Dohnal, J. (2011). Monitoring of recent mass movement activity in anthropogenic slopes of the Krušné Hory Mountains (Czech Republic). Natural Hazards and Earth System Sciences, 11, pp.1463–1473. https://doi.org/10.5194/nhess-11-1463-2011

Burda, J., Veselý, M., Řehoř, M., & Vilímek, V. (2018). Reconstruction of a large runout landslide in the Krušné hory Mts. (Czech Republic). Landslides, 15(3), pp.423–437. https://doi.org/10.1007/s10346-017-0881-0

Burda, J. (2014). Stability problems at the toe of the Krušné Hory Mts. Geomorphological Proceedings 12: State of geomorphological research, pp.16–17.

Burda, J. and Kycl, P. (2023). Selected findings from monitoring and slope stability evaluation of the ČSA open-pit mine. Příroda, 45, pp.141–164.

Burda, J., Mrlina, J. & Vilímek, V. (2022). Geodynamic phenomena in hazardous fault zones affected by extensive surface mining in Central Europe. Bulletin of Engineering Geology and the Environment, 81, 153. https://doi.org/10.1007/s10064-022-02650-x

Buša, J., et al. (2019). Hodnotenie zosuvného hazardu pomocou multivariačnej a bivariačnej štatistickej analýzy v Košickej kotline. Geografický časopis, 71(4), pp.383–405. http://dx.doi.org/10.31577/geogrcas.2019.71.4.20

Carrara, A. (1995). GIS Technology in Mapping Landslide Hazard. In: Carrara, A. and Guzzetti, F. (eds) Geographical Information Systems in Assessing Natural Hazards. Springer, pp.135–175. https://doi.org/10.1007/978-94-015-8404-3_8

Cehlár, M., Janočko, J., Šimková, Z., Pavlik, T., Tyulenev, M., Zhironkin, S., & Gasanov, M. (2019). Mine Sited after Mine Activity: The Brownfields Methodology and Kuzbass Coal Mining Case. Resources, 8(1), 21. https://doi.org/10.3390/resources8010021

Chen, T., Shu, J., Han, L., Tovele, G.S.V., & Li, B. (2023). Landslide mechanism and stability of an open-pit slope: The Manglai open-pit coal mine. Frontiers in Earth Science, 10, 1038499. https://doi.org/10.3389/feart.2022.1038499

ČUZK. (2016). Digitální model reliéfu České republiky 5. generace (DMR 5G). [online] Available at: https://geoportal.cuzk.cz/geoprohlizec/?wmcid=22517

Dahal, R. (2017). Landslide hazard mapping in GIS. Journal of Nepal Geological Society, 53, pp.63–91. https://www.nepjol.info/index.php/JNGS/article/view/23808/20182

Declercq, P-Y., Dusar, M., Pirard, E., Verbeurgt, J., Choopani, A., & Devleeschouwer, X. (2023). Post Mining Ground Deformations Transition Related to Coal Mines Closure in the Campine Coal Basin, Belgium, Evidenced by Three Decades of MT-InSAR Data. Remote Sensing, 15(3), 725. https://doi.org/10.3390/rs15030725

ESRI. (2022). ArcGIS Pro help. https://pro.arcgis.com/en/pro-app/2.7/help/main/welcome-to-the-arcgis-pro-app-help.htm

Europe Beyond Coal. (2018). Overview: national coal phase-out announcements in Europe. Brussels. https://thecoalhub.com/wp-content/uploads/2018/05/Overview-of-national-coal-phase-out-announcements-Europe-Beyond-Coal-Feb-2018.pdf

European Commission. (2019). The European Green Deal. COM (2019) 640 final. https://eur-lex.europa.eu/legal-content/EN/TXT/?uri=COM:2019:0640:FIN

Eurostat. (2022). Coal production and consumption statistics. https://ec.europa.eu/eurostat/statistics-explained/index.php?title=Coal_production_and_consumption_statistics.

Fathi Salmi, E., Nazem, M., & Karakus, M. (2016). Numerical analysis of a large landslide induced by coal mining subsidence. Engineering Geology, 217, pp.141–152. https://doi.org/10.1016/j.enggeo.2016.12.02 1

Galgóczi, B. (2019). Phasing out coal – a just transition approach. Working Paper 2019.04, Brussels: ETUI.

Görmar, F., Grillitsch, M., Hruška, V., Mihály, M., Nagy, E., Píša, J., & Stihl, L. (2022). Power relations and local agency: a comparative study of European mining towns. Urban Research & Practice, 16(4), pp. 558–581. https://doi.org/10.1080/17535069.2022.2051066

Haigh, M.J. (1992). Problems in the reclamation of coal-mine disturbed lands in Wales. International Journal of Surface Mining, Reclamation and Environment, 6(1), pp.31–37. https://doi.org/10.1080/09208119208944313

Hodasová, K. & Bednarik, M. (2021). Effect of using various weighting methods in a process of landslide susceptibility assessment. Natural Hazards, 105, pp.481–499. https://doi.org/10.1007/s11069-020-04320-1

IPCC. (2018). Special Report: Global Warming of 1.5°C. Intergovernmental Panel for Climate Change. https://www.ipcc.ch/sr15

Kadirhodjaev, A., Prima R.K., Chang-Wook L., & Saro L. (2018). Analysis of the relationships between topographic factors and landslide occurrence and their application to landslide susceptibility mapping: a case study of Mingchukur, Uzbekistan. Geosciences Journal, 22, pp.1053–1067. https://link.springer.com/article/10.1007/s12303-018-0052-x

Kalsnes, B. & Capobianco, V. (2022). Use of Vegetation for Landslide Risk Mitigation. In: Kondrup, C. Climate Adaptation Modelling. Springer Climate. Springer, Cham. https://doi.org/10.1007/978-3-030-86211-4_10

Karan, S.K., Samadder, S.R., & Maiti, S.K. (2016). Assessment of the capability of remote sensing and GIS techniques for monitoring reclamation success in coal mine degraded lands. Journal of Environmental Management, 182, pp.272–283. https://doi.org/10.1016/j.jenvman.2016.07.070

Kohnke, H. (1950). The Reclamation of Coal Mine Spoils. Advances in Agronomy, 2, pp.317–349. https://doi.org/10.1016/S0065-2113(08)60768-3

Malkovský, M. (1985). Geologie severočeské hnědouhelné pánve a jejího okolí. Praha: Academia.

Marek, J. (2006). Jezeří znovu v ohrožení? (Část II.). Geotechnika, 1, pp.3–13.

Mert, Y. (2019). Contribution to sustainable development: Re-development of post-mining brownfields. Journal of Cleaner Production, 240, p.118212. https://doi.org/10.1016/j.jclepro.2019.118212

Meten, M., Netra PB., & Ryuichi Y. (2015). Effect of Landslide Factor Combinations on the Prediction Accuracy of Landslide Susceptibility Maps in the Blue Nile Gorge of Central Ethiopia. Geoenvironmental Disasters, 2(1), 9. https://doi.org/10.1186/s40677-015-0016-7

Mühldorf, J. (1981). Komořany II. C – Jezeří. – Ms. Záv. zpr.; depon. in: Stavební geologie n. p., Praha.

Pasqualetti, M.J. & Frantál, B. (2022). The evolving energy landscapes of coal: Windows on the past and influences on the future. Moravian Geographical Reports, 30(4), pp.228–236. https://doi.org/10.2478/mgr-2022-0015

Reanud, V., Al Heib, M., & Burda, J. (2022). 3D large-scale numerical model of open-pit lake slope stability—case study of Lake Most. Bulletin of Engineering Geology and the Environment, 81, 282. https://doi.org/10.1007/s10064-022-02771-3

Reed, M. & Kite, S. (2020). Peripheral gully and landslide erosion on an extreme anthropogenic landscape produced by mountaintop removal coal mining. Earth Surface Processes and Landforms, 45, pp.2078–2090. https://doi.org/10.1002/esp.4867

Rybář, J. (1996). Hodnocení výsledků kontrolního sledování bočních svahů lomu ČS. armády v období 1983-1996. Závěrečná zpráva o řešení grantového projektu GA ČR: 205/94/1769, ÚSMH AV ČR, Praha, 10 s.

Rybář, J. & Novotný, J. (2005). Vliv klimatogenních faktorů na stabilitu přirozených a antropogenních svahů. Zpravodaj Hnědé uhlí, 3, pp.13–28.

Rybář, J. (2006). Vliv klimatu na vývoj různých typů svahových pohybů. Zprávy o geologických výzkumech, pp.90–92.

Reichenbach, P., Rossi, M., Malamud, B.D., Mihir, M., & Guzzetti, F. (2018). A review of statistically-based landslide susceptibility models. Earth-Science Reviews, 180, pp.60–91. https://doi.org/10.1016/j.earscirev.2018.03.001

Segoni, S., Pappafico, G., Luti, T., & Filippo C. (2020). Landslide susceptibility assessment in complex geological settings: sensitivity to geological information and insights on its parameterization. Landslides, 17, pp.2443–2453. https://doi.org/10.1007/s10346-019-01340-2

Silalahi, F.E.S., Pamela, Arifianti, Y., & Fahrul H. (2019). Landslide susceptibility assessment using frequency ratio model in Bogor, West Java, Indonesia. Geoscience Letters, 6, 10. https://doi.org/10.1186/s40562-019-0140-4

Stottmeister, U., Mudroch, A., Kennedy, C., Matiova, Z., Sanecki, J., & Svoboda, I. (2002). Reclamation and Regeneration of Landscapes after Brown Coal Open-cast Mining in Six Different Countries. In: Mudroch, A., Stottmeister, U., Kennedy, C. and Klapper, H. Remediation of Abandoned Surface Coal Mining Sites. Environmental Engineering. Springer, Berlin, Heidelberg. https://doi.org/10.1007/978-3-662-04734-7_2

Tokgöz, N. (2010). Case study of the Agacli landslide–gully complex during post-coal-mining reclamation and afforestation. Environmental Earth Sciences, 59, pp.1559–1567. https://doi.org/10.1007/s12665-009-0141-2

Ujjwal, S., Singh, P., & Meena, S. (2020). Landslide susceptibility assessment in a lesser Himalayan road corridor (India) applying fuzzy AHP technique and earth-observation data. Geomatics, Natural Hazards and Risk, 11, pp.2176–2209. https://doi.org/10.1080/19475705.2020.1836038

Valeš, J. (1998). Řešení stabilitních problémů na jižním úpatí Krušných hor. In: Valašek, V. (ed.) 45 let Výzkumného ústavu pro hnědé uhlí v Mostě. Most: Výzkumný ústav pro hnědé uhlí a.s., pp.95–100.

Valvoda, P., Veselý, M., Fultner, J., Žižka, L., & Burda, J. (2020). Stabilitní studie k zatápění lomu ČSA (dodatek – posouzení hladiny 230 m). Závěrečná zpráva, arch. č. Výzkumný ústav pro hnědé uhlí a.s.: GH-024/20.

Van Westen, C.J., Rengers, N., Terlien M.T.J., & Soeters, R. (1997). Prediction of the occurrence of slope instability phenomena. Geologische Rundschau, 84, pp. 404–414. https://doi.org/10.1007/s005310050149

Van Westen, C.J., Castellanos E., & Kuriakose S.L. (2008). Spatial data for landslide susceptibility, hazard, and vulnerability assessment: An overview. Engineering Geology, 102(3–4), pp. 112–131. https://doi.org/10.1016/j.enggeo.2008.03.010

Wirth, P., Černič Mali, B., & Fischer, W. (2012). Post-Mining Regions in Central Europe: Problems, Potentials, Possibilities. München: oekom verlag.

Yalcin, A. (2008). GIS-based landslide susceptibility mapping using analytical hierarchy process and bivariate statistics in Ardesen (Turkey): Comparisons of results and confirmations. Catena, 72, pp.8–12. https://doi.org/10.1016/j.catena.2007.01.003

Yang, D., Qiu, H., Ma, S., Liu, Z., Du, C., Zhu, Y., & Cao, M. (2022). Slow surface subsidence and its impact on shallow loess landslides in a coal mining area. Catena, 209(1), 105830. https://doi.org/10.1016/j.catena.2021.105830

Yong, C., Jinlong, D., Fei, G., Bin T., Tao Z., Hao F., Li W., & Qinghua W. (2022). Review of landslide susceptibility assessment based on knowledge mapping. Stochastic Environmental Research and Risk Assessment, 36, pp.2399–2417. https://doi.org/10.1007/s00477-021-02165-z

Xiao, W., Hu, Z., & Fu, Y. (2014). Zoning of land reclamation in coal mining area and new progresses for the past 10 years. International Journal of Coal Science & Technology, 1, pp.177–183. https://doi.org/10.1007/s40789-014-0024-3

Zmítko, J. (1983). Fosilní sesuv při podkrušnohorském výchozu pánve. Hnědé uhlí, 6, pp.12–24.

Žižka, L. & Halíř, J. (2010). Hydrogeological circumstances of the Quaternary cover in the Central part of the Most Basin. Model CARE, pp.583–585.